Effective Electrochemically Controlled Process for Perchlorate Removal Using Poly(aniline-*co-o*-aminophenol)/Multiwalled Carbon Nanotubes

Ya Zhang, Xuanming Liu, Qin Li

State Key Laboratory of Pollution Control and Resource Reuse, School of the Environment, Nanjing University, Nanjing 210093, People's Republic of China
Correspondence to: Q. Li (E-mail: qli@nju.edu.cn)

ABSTRACT: The study on perchlorate removal from simulated wastewater was carried out using a conducting copolymer poly(aniline-*co-o*-aminophenol) (PANOA) polymerized on multiwalled carbon nanotubes (MWNTs)-modified glassy carbon (GC) electrode. The cyclic voltammograms demonstrated that the PANOA/MWNTs GC electrode in a NaCl solution containing NaClO$_4$ had a good redox activity, reversibility, and stability in a wide range of pHs tested (from pH <1 to 9.0). The ratio of ClO$_4^-$/Cl$^-$ in PANOA/MWNTs was up to 80.8%, which was 10.0% in the solution, indicating that PANOA/MWNTs had a relatively high affinity to perchlorate. The result of X-ray photoelectron spectroscopy revealed a fact that Cl$^-$ ions can be strongly adsorbed on MWNTs, which resulted in an improvement in the electrical activity of PANOA and perchlorate removal. Therefore, it is possible to develop a green process for removing perchlorate from wastewater using PANOA/MWNTs. © 2012 Wiley Periodicals, Inc. J. Appl. Polym. Sci. 000: 000–000, 2012

INTRODUCTION

Perchlorate has emerged as a significant threat to ground water, drinking water, and soil.[1–3] Recently, Dasgupta et al.[4] have first compared a woman's daily intake of iodine and perchlorate in her breast milk, concluding that 9 out of 13 infants received three times higher perchlorate than the NAS recommendation. It has been reported that perchlorate can displace iodide from the thyroid gland, block the uptake of iodine in the thyroid.[5] The primary source of man-made perchlorate contamination is wide use of ammonium perchlorate as an oxidant in rockets and missiles. Perchlorate salts are also commonly used in munitions, fireworks, lithium batteries, and air bags.[6–8] Fertilizers could be a source for perchlorate accumulation in the food chain.

Perchlorate ions are nonvolatile, highly soluble, and kinetically inert in the dilute aqueous solution. As a result, conventional water treatment technologies such as carbon adsorption, ultrafiltration, and advanced oxidation are ineffective for removing perchlorate from water.[1,9] Therefore, many new strategies are tried for the investigation and application of perchlorate removal from contaminated water. Catalytic reduction of ClO$_4^-$ using organic sulfides and oxorhenium (V) complexes and titanous ions has been reported to be successful,[1,10] but the high cost and ineffectiveness in treatment of low levels of ClO$_4^-$ render the technologies questionable. Because of its high efficiency and minimal impact on water quality, selective ion exchange is one of the preferred treatment technologies for removing low levels of perchlorate from contaminated water. However, the exceptionally high affinity of ClO$_4^-$ makes the resin regeneration with conventional NaCl brine extremely difficult and costly for practical applications.[11] Among new strategies, electrochemical treatment is a promising technique.[12,13] Recently, Lin et al.[14] reported the electrically controlled anion exchange based on polypyrrole. This study aroused an upsurge in investigation on perchlorate removal for its low cost, no secondary wastes, and simple operation conditions.

In recent years, conducting polymers have been attracting significant interest owing to high conductibility, good electrochemical activity, and stability in aqueous solutions.[15,16] Redox properties of the conducting polymer can be fully exploited to lead a green ion exchange process. The oxidation of the conducting polymer is accompanied with incorporation of anions of the solution into the conducting polymer, that is doping; the reduction of the conducting polymer is accompanied with release of anions from the conducting polymer into the solution, that is dedoping. Therefore, on the basis of doping and dedoping

principle, the conducting polymer would be used to remove perchlorate from contaminated water. Among conducting polymers, poly(aniline-*co-o*-aminophenol) (PANOA) has good redox activity from pH <1.0 to 11.0,[17,18] which has been used to remove perchlorate[19] and arsenate[20] from aqueous solution.

The capacity of perchlorate removal is mainly dependent on the electrochemical activity of the conducting polymer in the contaminated water. Carbon nanotubes are one of the novel materials with exceptional physicochemical, optical, and mechanical properties.[21,22] Multiwalled carbon nanotubes (MWNTs) and their derivatives and hybrids have a wide variety of applications, including composite construction materials,[23] microelectronics,[24] and energy storage.[25] Thus, it is expected that the MWNTs could increase the surface area of electrode and enhance the electrical activity and stability of PANOA.

In this study, PANOA was electrochemically synthesized on MWNTs glassy carbon (GC) electrode; PANOA/MWNTs was characterized by cyclic voltammetry, Fourier transform infrared spectroscopy (FTIR) and electron spin resonance (ESR) spectra, and X-ray photoelectron spectroscopy (XPS); perchlorate could be effectively removed from aqueous solution through electrochemically controlled process using PANOA/MWNTs.

EXPERIMENTAL

Materials

Sodium perchlorate (≥98%) was purchased from (Fluka, Switzerland). *N, N*-dimethylformamide (DMF), sodium chloride, *o*-aminophenol, and hydrochloric acid were of analytical reagent grade obtained from Shanghai Chemical (Shanghai, China). Aniline was distilled under reduced pressure before use. MWNTs (diameter, 20–40 nm) were purchased from Shenzhen Nanotech Port (NTP, Shenzhen, China). Doubly distilled water was used to prepare solutions.

Preparation of Working Electrodes

MWNTs were immersed in $3.5M$ HCl solution overnight to remove metal impurities and then sonicated in doubly distilled water bath for 1 h. The GC disk (diameter, 3 mm, CHI) electrode was polished with alumina slurry of 0.5 μm on polishing cloth with water as a lubricant, and then rinsed with distilled water, finally sonicated in doubly distilled water bath for 10 min. To prepare GC/MWNTs electrode, MWNTs were dispersed in DMF with the aid of ultrasonic agitation. The mixture of MWNTs–DMF (5 mg/mL, 5 μL) was introduced on the surface of the GC electrode substrate using a micropipette, and the solvent was evaporated at room temperature. The GC/MWNTs electrode was used for the synthesis of the PANOA.

Preparation of PANOA Films

An electrolytic cell for the synthesis of PANOA consisted of a GC/MWNTs working electrode, a platinum foil counter electrode, and a saturated calomel reference electrode (SCE). All potentials given here are referred to an SCE. PANOA was synthesized using the previously described chronoamperometry method.[19,20] The doped and dedoped PANOA samples were used for the measurements of IR and XPS spectra.
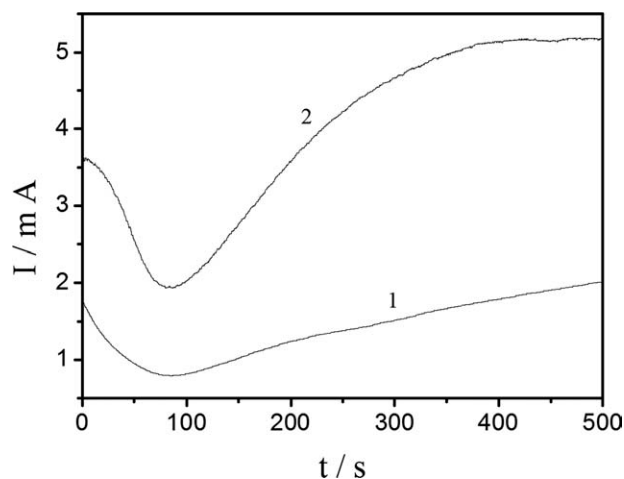

Figure 1. *I–t* curves in the electrolysis solution consisting of $0.3M$ aniline, 5.5 mM *o*-aminophenol, and $2.0M$ HCl, using GC/MWNTs electrode at a constant potential of 0.79 V, (1) quiescent solution; (2) stirred solution.

Instruments

The pH values of the solutions were determined by using a PXD-12 pH meter. Cyclic voltammetry (CV) and Chronoamperometry were performed on a Model CHI 407 electrochemical workstation. The FTIR spectra of PANOA samples were measured on a pressed pellet with KBr using a Bruker IFS 66/s spectrometer. The ESR measurements were carried out using a Bruker A300 spectrometer operating in *X*-band (9.862 GHz). The microwave power for the measurements of the copolymer samples in the solid state was as low as 0.20 mW and modulation amplitude was set at 1.0 G. The measurements of XPS of the samples were made on a Thermo ESCALAB 250 spectrometer with an Al Kα X-ray source (1486.6 eV). The samples were kept under vacuum of about 10^{-7} Pa on a sample holder. All binding energies were referenced to C 1s neutral carbon peak at 284.6 eV.

RESULTS AND DISCUSSION

Electrochemical Synthesis of PANOA

A standard electrolytic solution consisted of $0.30M$ aniline, 5.5 mM *o*-aminophenol and $2.0M$ HCl; the electrochemical copolymerization was carried out under a constant potential of 0.79 V. Curves 1 and 2 in Figure 1 show the *I–t* curves in the aforementioned electrolysis solution without and with stirring, respectively. The current in both curves decreases at the beginning of electrolysis. Then the current increases with time. The former is caused by both of the concentration polarization and of the formation of the PANOA film with lower conductivity than that of GC/MWNTs. For the electrolysis at a constant potential, the current is generally to decrease with time for a quiescent solution because of the concentration polarization around the electrode; and the current first degrees and then quickly approaches the steady-state value for the stirred solution. The current in Figure 1 increases with time after the beginning of electrolysis, which is caused by autocatalytic copolymerization as well as the electrochemical polymerization of aniline and the growth of the electroactive film. It is evident that the current on curve 2 is higher than that on curve 1 because the stir accelerates mass transfer in the solution, which
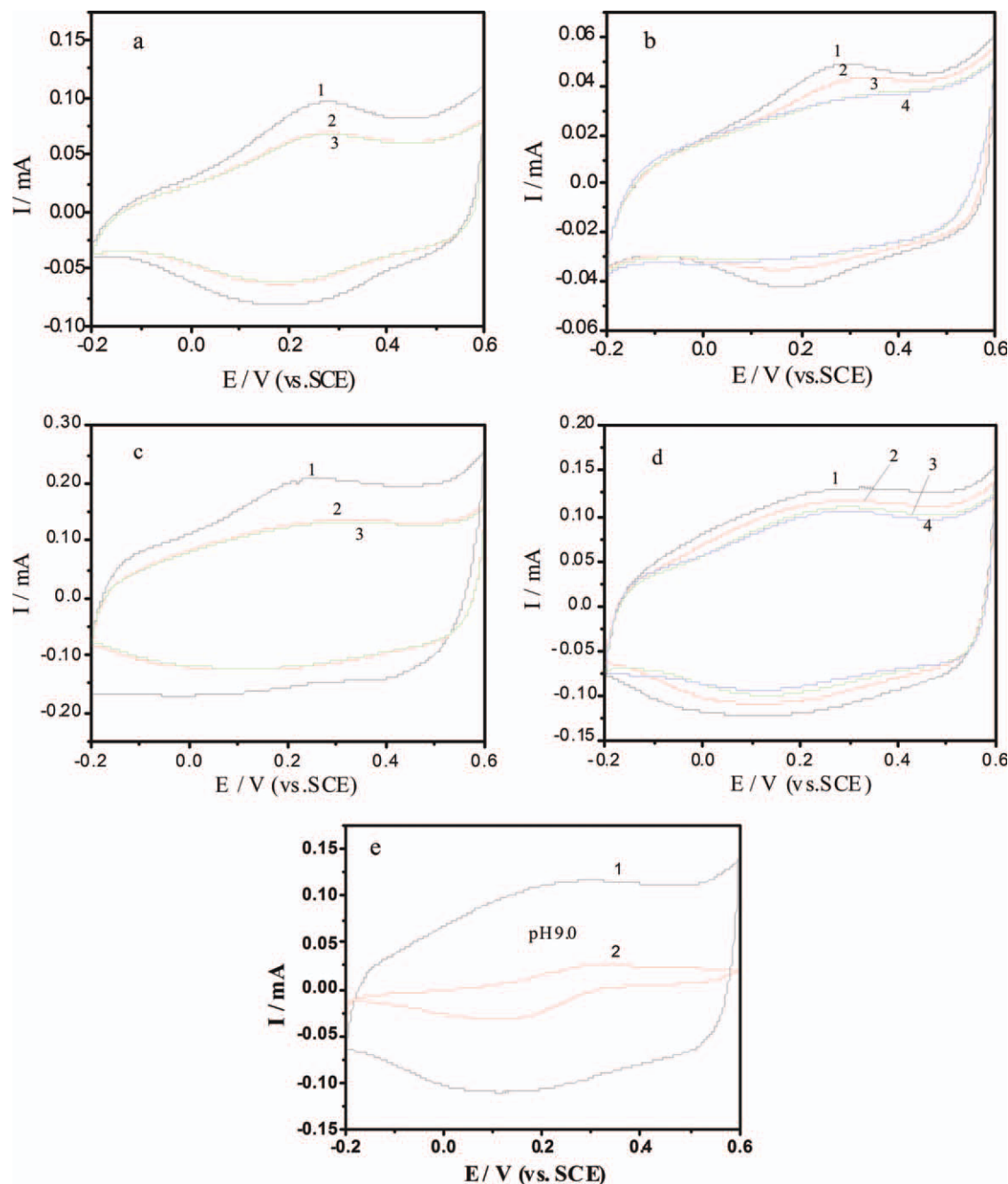
Figure 2. Cyclic voltammograms of PANOA deposited on the GC/MWNTs electrode, (a) in 0.10M NaCl solution of pH 5.7, (b) in 0.10M NaCl solution of pH 9.0, curves: (1) first cycle, (2) ninth cycle, and (3) tenth cycle. Cyclic voltammograms of PANOA deposited on the GC/MWNTs electrode in 0.10M NaCl solutions of pH 5.7 (c) and pH 9.0 (d) without and with different concentrations of NaClO$_4$, Curves: (1) without NaClO$_4$, (2) with 1.0 mM NaClO$_4$, (3) with 10.0 mM NaClO$_4$, (4) with 40.0 mM NaClO$_4$. (e) CVs of PANOA deposited on the GC (curve 2) and GC/MWNTs (curve 1) electrodes in 0.10M NaCl solution with 1.0 mM NaClO$_4$ of pH 9.0, respectively. Scan rate: 5 mV s^{-1}. [Color figure can be viewed in the online issue, which is available at wileyonlinelibrary.com.]

results in the increase of copolymerization rate. The result shown in Figure 1 demonstrates that the copolymerization rate is rather fast.

Redox Properties of PANOA

CV provides a quick and reliable approach to assess the redox properties of a conducting polymer. Figure 2(a, b) shows the

CV of PANOA deposited on GC/MWNTs electrode immersed in 0.10M NaCl solution with pH 5.7 and 9.0, respectively. As shown in Figure 2(a, b), electroactive decay happened from the first cycle to the ninth cycle, caused by the pH difference between the solution and the inner site of PANOA. This is because PANOA was synthesized in 2.0M HCl solution, which needs time to reach the pH equilibrium between the inside of
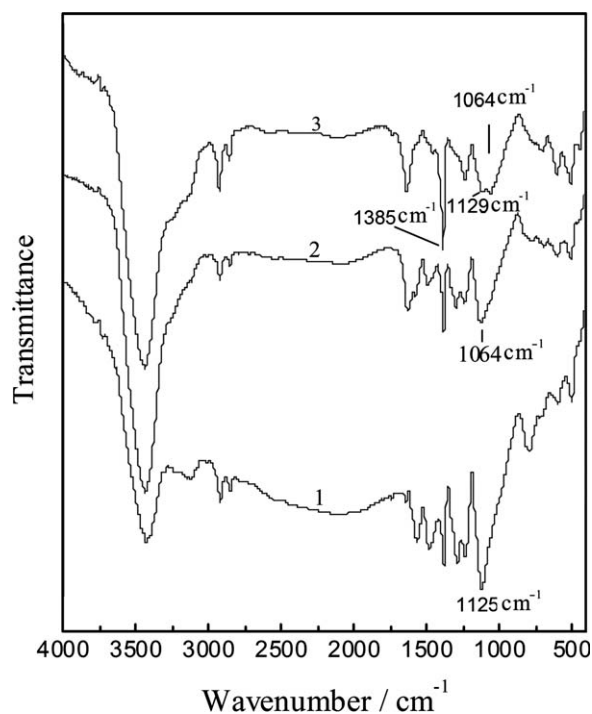
Figure 3. IR spectra of PANOA at different states: (1) as-prepared PANOA at the oxidized state, PANOA oxidized in the solution consisting of 0.10M NaCl and different concentrations of NaClO$_4$, (2) 10.0 mM NaClO$_4$, and (3) 40.0 mM NaClO$_4$.

the PANOA film and the bulk solution. However, the CV of the tenth cycle is almost overlapped on the ninth cycle, indicating that the electrochemical redox of PANOA is reversible and PANOA reaches quickly a stable state. Therefore, the PANOA is conductive and reversible in redox properties in a wide pH range from <1 to 9.0.

Influence of ClO$_4^-$ Ions on the Cyclic Voltammograms

Curves 1–4 in Figure 2(c) (pH 5.7) and Figure 2(d) (pH 9.0) show the CVs of PANOA deposited on the GC/MWNTs electrode in 0.10M NaCl solution with varying perchlorate concentrations (0.0–40.0 mM). There is an oxidation peaks at 0.24 V and a broad reduction potential plateau on curve 1. The oxidation peak at 0.24 V on curve 1 corresponds to the oxidation of leucoemeraldine to emeraldine of PANOA, which is accompanied by the exchange of anions between the PANOA film and the solution as well as polyaniline based on the experimental result of the electrochemical quartz crystal microbalance (EQCM).[26] The experimental result revealed a fact that the oxidation peak at 0.24 V on curve 1 shifts toward more positive potentials and meanwhile the broadness of the reduction plateau becomes narrower as the concentration of ClO$_4^-$ increases. The former is strongly indicative of the exchange of anions because the peak potential depends on the concentration of NaClO$_4$. Therefore, this result also supports the result of EQCM. In another words, the exchange of anions during the redox process of polyaniline or polyaniline derivative can also be detected using CV based on the differences in the mobility and sizes of anions. It is well known that the plot of I–E on the CV

is equivalent to the plot of current versus time. That is, the area of the CV represents the quantity of electricity. Therefore, the area of the CV can also be regarded as the redox activity of the conducting polymer at a given condition. Figure 2(e) shows the CVs of PANOA deposited on the GC (curve 2) and GC/MWNTs (curve 1) electrodes in a 0.10M NaCl solution with 1.0 mM NaClO$_4$ of pH 9.0, respectively. We found that the area in the potential range of −0.2 to 0.6 V on curve 1 [Figure 2(e)] is much larger than that on curve 2, which indicates that the ion exchange capacity of PANOA deposited on the GC/MWNTs electrode is larger than that of PANOA deposited on the GC electrode. It is clear that the redox activity of PANOA deposited on the GC/MWNTs electrode is pronouncedly improved compared to that of PANOA deposited on the GC electrode because of the large surface area and conductance of MWNTs.

FTIR Spectra

The FTIR spectrum is a good tool to identify whether the ClO$_4^-$ ions are incorporated in the PANOA or not, because the ClO$_4^-$ has its characteristic frequencies in the ranges of 1100–1025 cm^{-1}.[27] Curves 1–3 in Figure 3 show the FTIR spectra of PANOA synthesized in the HCl solution and doped in 0.10M NaCl solution containing 10.0 and 40.0 mM NaClO$_4$ of pH 5.7, respectively. The details of the IR spectrum of PANOA have been reported elsewhere[17,18]; therefore, no reiterating a statement is necessary here. However, we are interested in the absorption peak at 1125 cm^{-1} on curve 1 in Figure 3, which is caused by aromatic C—H in-plane bending vibrations (1250–1025 cm^{-1}).[28] This is because its wavenumber is close to the frequency range of ClO$_4^-$ as mentioned previously. As shown in Figure 3, a peak at 1129 cm^{-1} with a shoulder at 1064 cm^{-1} appears on curve 2, which is in good agreement with that of the IR spectrum of polyaniline synthesized in perchloric acid solution.[29] The peaks at 1129 and 1064 cm^{-1} on curve 3 are similar to that on curve 2, but the relative transmittance on curve 3 is obviously higher than that on curve 2, which indicates that the peak transmittance becomes higher as the concentration ratio of ClO$_4^-$/Cl$^-$ increases. Therefore, the absorption peak at 1064 cm^{-1} on curves 2 and 3 is attributed to ClO$_4^-$, which is strong evidence for that the ClO$_4^-$ ions were incorporated in PANOA during the oxidation process. In addition, a strong peak at 1385 cm^{-1} appears on each curve in Figure 3, which is attributed to the deformation vibrations of the C—O—H bond in the copolymer, as a peak at 1400 cm^{-1} appears in the IR spectrum of o-aminophenol[30] and the IR spectra of phenols have a absorption peak at 1390–1310 cm^{-1}.[28] Therefore, the appearance of the absorption peak at 1385 cm^{-1} demonstrates that the PANOA chain contains o-aminophenol unit.

ESR Spectra

As discussed previously, the anodic peak potential of doped PANOA shifts toward the positive direction is caused by the electrode polarization owing to the large size and slow mobility of ClO$_4^-$. After the oxidation, the ClO$_4^-$ ions replaced partially Cl$^-$ ions in the PANOA, which may influence the properties of the radicals of the copolymer. It is well known that ESR is an extremely sensitive technique for the detection of radicals. Therefore, the ESR technique was used here to approach the
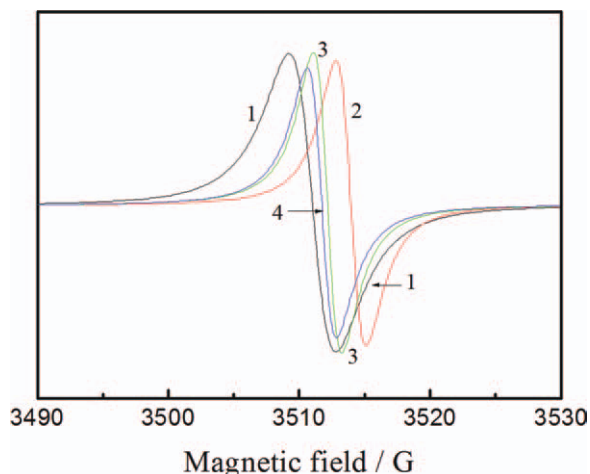
Figure 4. ESR spectra of the PANOA at different states: (1) as-prepared PANOA at the oxidized state, PANOA oxidized in the solution consisting of 0.10M NaCl and different concentrations of NaClO$_4$, (2) 1.0 mM NaClO$_4$, (3) 10.0 mM NaClO$_4$, and (4) 40.0 mM NaClO$_4$. [Color figure can be viewed in the online issue, which is available at wileyonlinelibrary.com.]

effect of ClO$_4^-$ ions doped into the PANOA on the ESR signal. Figure 4 shows the ESR spectra of the PANOA synthesized in the HCl medium (curve 1) and doped in the solution consisting of 0.10 M NaCl with different concentrations of ClO$_4^-$ (curves 2–4). All resulting copolymer samples used here are at 0.60 V, indicating at the same oxidation state. As shown in Figure 4, each spectral line consists of a symmetric signal. The values of the peak-to-peak line width ΔH_{PP} of curves 1–4 are 3.62, 2.44, 2.25, and 2.15 G, respectively. The ΔH_{PP} value of the ESR signal is characteristic of a radical itself. The ΔH_{PP} value of the PANOA synthesized in the HCl solution, that is only doped Cl$^-$ ions, is the largest among the tested samples, and then decreases as the concentration of ClO$_4^-$ in the doping solution increases. This indicates that the amount of ClO$_4^-$ in the PANOA increases with increasing the concentration of ClO$_4^-$ in the doping solution. This result is in good agreement with the result of FTIR spectra of the PANOA samples. Also, the ESR spectra presented here give strong evidence that the PANOA can effectively remove ClO$_4^-$ ions in the solution containing the concentration of ClO$_4^-$ as low as 1.0 mM.

XPS Spectra

In this study, XPS was used to study the surface composition of PANOA and to detect simultaneously both Cl$^-$- and ClO$_4^-$- doped PANOA. This is because XPS is a very useful tool to distinguish the valence electrons of atom under different chemical environments based on the change in the binding energy of the core electrons, that is chemical shift which is dependent on the nature and number of neighboring atoms. Therefore, it is expected that the binding energy of Cl 2p electrons of Cl$^-$ lower than that in ClO$_4^-$, as oxygen is more electronegative than chlorine. Figure 5(a) shows the XPS spectra of the PANOA copolymers obtained at different conditions. Curve 1 in Figure 5(a) is the XPS spectrum of the copolymer synthesized in the HCl solution at the oxidation state; curves 2 and 3 are the XPS spectra

of the copolymer doped in 0.10M NaCl solution containing 1.0 and 10.0 mM NaClO$_4$ of pH 5.7, respectively; curve 4 is the XPS spectrum of the dedoped PANOA. As shown in Figure 5(a), all PANOAs are composed of C, N, O, and Cl. It is notable that two distinguishable weak peaks around 200 eV attributed to Cl 2p appear on curve 3 in Figure 5(a). This gives us a significant hint that the chemical shift of Cl 2p occurs. To study further, the high-resolution XPS spectra of the individual Cl in above PANOAs are shown in Figure 5(b). Four Cl 2p peaks at
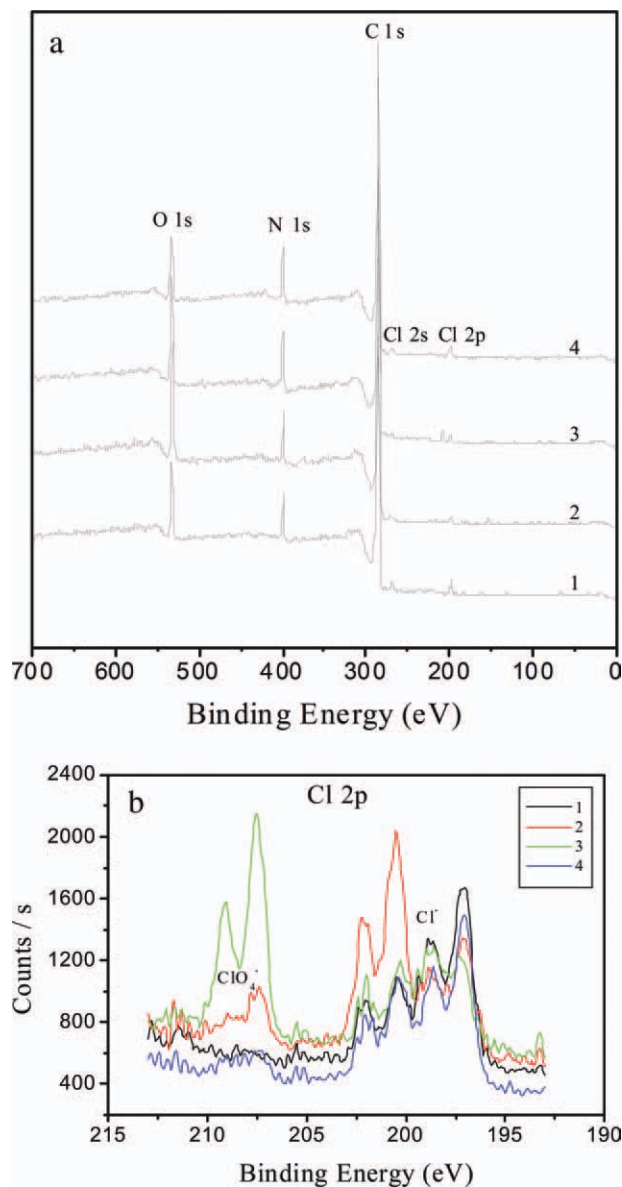

Figure 5. (a) XPS spectra of PANOA at different states: (1) as-prepared PANOA at the oxidized state; (2), (3) PANOA obtained by oxidation in the solution consisting of 0.10M NaCl and 10.0 and 40.0 mM NaClO$_4$, respectively; (4) dedoped PANOA. (b) XPS spectra of high-resolution scans of Cl: (1) as-prepared PANOA at the oxidized state; (2), (3) PANOA obtained by oxidation in the solution consisting of 0.10M NaCl and 10.0 and 40.0 mM NaClO$_4$, respectively; (4) dedoped PANOA. [Color figure can be viewed in the online issue, which is available at wileyonlinelibrary.com.]

Table I. Surface Composition (in at.%) of PANOAs at Different States

| Samples | C_{1s} | O_{1s} | N_{1s} | Cl_{2p} | | Cl/N (%) | ClO_4^-/Cl^- (%) |
				Cl^-	ClO_4^-		
1	79.6	10.4	8.25	1.76	0.00	21.3	0.00
2	80.1	8.21	9.97	1.54	0.20	17.5	13.0
3	75.8	12.9	9.13	1.20	0.97	23.8	80.8
4	79.1	10.0	9.19	1.58	0.15	18.8	9.49

197, 199, 201, and 202 eV appear on each curve in Figure 5(b). Generally, Cl shows two Cl $2p_{1/2}$ peaks, located at about 197 and 199 eV.[31] To define the two new peaks, MWNTs were immersed into the 1.0M HCl solution for 1 h, then washed with doubly distilled water, and then finally dried at 102°C before the determination of the XPS spectrum. Its XPS spectrum demonstrated that two peaks also located at 201 and 202 eV (the spectrum omitted here). It is clear that two peaks at 201 and 202 eV in Figure 5(b) are caused by the interaction between MWNTs and Cl^- ions. A possible explanation for this is that Cl^- ions were strongly adsorbed on MWNTs, which results in the chlorine valence electrons shift toward the carbon atom. This would cause the influence of chlorine nucleus on Cl 2p electron to increase, and its effect would be to bind the Cl 2p electron more strongly to chlorine nucleus and hence increases the Cl 2p core binding energy. In addition, two extra Cl 2p peaks at 207 and 209 eV on curves 2 and 3 that are attributed to the Cl in ClO_4^- ions, which indicates that ClO_4^- ions can be successfully doped into PANOA. This is owing to the fact that the chlorine valence electrons in ClO_4^- shift somewhat toward the oxygen atom. This would cause the influence of chlorine nucleus on Cl 2p electron to increase, and its effect would be to bind the Cl 2p electron more strongly to chlorine nucleus and hence increased the Cl 2p core binding energy. Comparing with curves 2, a significant increase in intensity of the peak attribute to ClO_4^- ions is detected on curve 3, indicating that the doped amount of ClO_4^- in PANOA increases as the concentration of ClO_4^- increases in the solution used for the doping of PANOA. Curve 4 in Figure 5(b) clearly demonstrates that only a small fraction of Cl^- ions remained in PANOA, but ClO_4^- was hardly detected, indicating that most anions were removed from the PANOA after it was reduced.

Table I summarizes the surface composition of PANOAs at different states. Samples 1–4 are as-prepared PANOA at the oxidation state, doped PANOA obtained by oxidation in a 0.10M NaCl solution (pH 5.7) consisting of 1 and 10.0 mM NaClO$_4$, and dedoped PANOA, respectively. The doping levels (Cl/N) of samples 1–4 are 21.3, 17.5, 23.8, and 18.8%, respectively. The varying doping levels of samples 1–4 are ascribed to the difference in solution ionic strength and pH. As summarized in Table I, the ratios of ClO_4^-/Cl^- of samples 2 and 3 are 13.0 and 80.8%, respectively, which are 1.0 and 10.0% in the tested solution. The atomic ratio of ClO_4^-/Cl^- is much higher than that in our previous study,[18] which was 26.3% in a 0.1M NaCl (pH 5.7) containing 10 mM NaClO$_4$. The result shows that PANOA deposited on the GC/MWNTs electrode has a high affinity to

ClO_4^-, which indicates that the MWNTs can remarkably enhance the electrochemical activity.

Results from both IR and XPS spectra demonstrate that ClO_4^- ions can be successfully doped into PANOA; PANOA has a much higher affinity for perchlorate over chloride with the aid of MWNTs.

CONCLUSIONS

Results from IR, ESR, and XPS spectra demonstrate that PANOA can be used to remove perchlorate ions in the solution. Compared with PANOA, PANOA/MWNTs can remove perchlorate ions more effectively, which is confirmed by the CVs and XPS determination. As expected, the PANOA/MWNTs has fairly good redox properties and affinity to perchlorate over chloride in a wide range of pHs. All these characteristics suggest that PANOA and other conducting polymers will likely lead to even more exciting future discoveries and intriguing applications.

REFERENCES

1. Susarla, S.; Collette, T. W.; Garrison, A. W.; Wolfe, N. L.; Mccutcheon, S. C. *Environ. Sci. Technol.* **1999,** *33*, 3469.
2. Yoon, I. H.; Meng, X. G.; Wang, C.; Kim, K. W.; Bang, S.; Choe, E. Y.; Lippincott, L. J. *Hazard. Mater.* **2009,** *164*, 87.
3. Kirk, A. B.; Smith, E. E.; Tian, K.; Anderson, T. A.; Dasgupta, P. K. *Environ. Sci. Technol.* **2003,** *37*, 4979.
4. Dasgupta, P. K.; Kirk, A. B.; Dyke, J. V.; Ohira, S. *Environ. Sci. Technol.* **2008,** *42*, 8115.
5. Moreno, J. C.; Bikker, H.; Kempers, M. J. E.; Van Trotsenburg, A. S. P.; Baas, F.; De Vijlder, J. J. M.; Vulsma, T.; Ris-Stalpers, C. N. *Engl. J. Med.* **2002,** *347*, 95.
6. ITRC (Interstate Technology & Regulatory Council). Perchlorate: Overview of Issues, Status, and Remedial Options; PERCHLORATE-1; Perchlorate Team, ITRC: Washington, DC, 2005; Available at http//www.itrcweb.org.
7. Magnuson, M. L.; Urbansky, E. T.; Kelty, C. A. *Anal. Chem.* **2000,** *72*, 25.
8. Sturchio, N. C.; Hatzinger, P. B.; Arkins, M. D.; Suh, C.; Heraty, L. J.; Environ. *Sci. Technol.* **2003,** *37*, 3859.
9. Logan, B. E. *Biorem. J.* **1998,** *2*, 69.
10. Abu-Omar, M. M.; Mcpherson, L. D.; Arias, J.; Bereau, V. M. *Angew. Chem. Int. Ed. Engl.* **2000,** *39*, 4310.
11. Gu, B. H.; Brown, G. M.; Maya, L.; Lance, M. J.; Moyer, B. A. *Environ. Sci. Technol.* **2001,** *35*, 3363.

12. Hatfield, T. L.; Kleven, T. L.; Pierce, D. T. *J. Appl. Electrochem.* **1996,** *26*, 567.

13. Lang, G. G.; Horanyi, G. *J. Electroanal. Chem.* **2003,** *552*, 197.

14. Lin, Y. H.; Cui, X. L.; Bontha, I. *Environ. Sci. Technol.* **2006,** *40*, 4004.

15. Khatoon, A.; Khalid, M.; Mohammad, F. *J. Appl. Polym. Sci.* **2008,** *108*, 3769.

16. Koysuren, O.; Du, C. S.; Pan, N.; Bayram G. *J. Appl. Polym. Sci.* **2009,** *113*, 1070.

17. Zhang, J.; Shan, D.; Mu, S. L. *J. Polym. Sci. Polym. Chem.* **2007,** *45*, 5573.

18. Mu, S. L. *Synth. Met.* **2004,** *143*, 259.

19. Zhang, Y.; Mu, S. L.; Deng, B. L.; Zheng, J. Z. *J. Electroanal. Chem.* **2010,** *641*, 1.

20. Zhang, Y.; Li, Q.; Sun, L.; Zhai, J. P. *J. Electroanal. Chem.* **2009,** *636*, 47.

21. Liu, J.; Rinzler, A. G.; Dai, H. J.; Hafner, J. H.; Bradley, R. K.; Boul, P. J.; Lu, A.; Iverson, T.; Shelimov, K.; Huffman, C. B.; Rodriguez-Macias, F.; Shon, Y. S.; Lee, T. R.; Colbert, D. T.; Smalley, R. E. *Science* **1998,** *280*, 1253.

22. Mauter, M. S.; Elimelech, M. *Environ. Sci. Technol.* **2008,** *42*, 5843.

23. Ajayan, P. M.; Stephan, O.; Colliex, C.; Trauth, D. *Science* **1994,** *265*, 1212.

24. Rosen, R.; Simendinger, W.; Debbault, C.; Shimoda, H.; Fleming, L; Stoner, B.; Zhou, O. *Appl. Phys. Lett.* **2000,** *76*, 1668.

25. Che, G. L.; Lakshmi, B. B.; Fisher, E. R.; Martin, C. R. *Nature* **1998,** *393*, 346.

26. Orata, D.; Buttry, D. A. *J. Am. Chem. Soc.* **1987,** *109*, 3574.

27. Nakanishi, K.; Solomon, P. H. Infrared Absorption Spectroscopy, 2nd ed.; Holden-Day, Inc.: San Francisco, **1977;** p 56.

28. Lambert, J. B.; Shurvell, H. F; Lightner, D. A.; Cooks, R. G. Organic Structural Spectroscopy; Prentice Hall: Upper Saddle River, NJ, **1998;** p 214.

29. Mu, S. L.; Kan, J. Q. *Synth. Met.* **1998,** *98*, 51.

30. Standard Infrared Grating Spectra, Sadtler Research Laboratories Inc.; Philadelphia, **1971;** Vols. 21–22, 21112 K.

31. Naoi, K.; Smyrl, W. H. *Chem. Mater.* **1992,** *4*, 988.